Acta Cryst. (1975). B31, 574

High-Pressure MnP_4, a Polyphosphide with Mn–Mn Pairs

BY W. JEITSCHKO AND P. C. DONOHUE

Central Research Department, E. I. du Pont de Nemours and Company, Wilmington, Delaware* 19898, *U.S.A.*

(*Received* 26 *July* 1974; *accepted* 23 *September* 1974)

The new compound MnP_4 was prepared by reaction of the elemental components at pressures of 30–55 kbar in a tetrahedral anvil high-pressure device. It is a diamagnetic semiconductor with an activation energy of 0·14 eV and crystallizes with space group $C2/c$, $a=10{\cdot}513$ (1), $b=5{\cdot}0944$ (4), $c=21{\cdot}804$ (2) Å, $\beta=94{\cdot}71$ (1)°, and $Z=16$. The structure was determined from single-crystal counter data by Patterson and Fourier methods and refined to a conventional R of 0·051 for 1765 reflections. The Mn atoms are in octahedral P coordination, and the P atoms are tetrahedrally coordinated by Mn and P atoms. The Mn atoms have formal oxidation number 2+ (d^5 configuration). Four MnP_6 octahedra share edges to form a linear array of four Mn atoms. The Mn atoms are displaced from the centers of the octahedra toward one another to form pairs with a resulting Mn–Mn bonding distance of 2·941 Å, thus accounting for the diamagnetism. Average Mn–P and P–P distances are 2·282 and 2·225 Å, respectively. MnP_4 can be described as an eight-layer stacking variant of the two-layer CrP_4 structure, although bonding within and between the layers is of equal strength. Qualitative MO bonding models for the MnP_4 and CrP_4 structures are presented that allow rationalization of magnetic and conductive properties. A similar bonding proposal is made for the marcasite and arsenopyrite structures which, as is the case for CrP_4 and MnP_4, have TP_6 octahedra linked *via* edges, with transition metal atoms forming infinite strings and pairs, respectively.

Introduction

Investigations of the Mn–P system at ambient pressure resulted in the characterization of Mn_3P, Mn_2P, and MnP (Årstad & Nowotny, 1937; Rundqvist, 1962). Between MnP and P, only the phase MnP_3 was found by Biltz, Wiechmann & Meisel (1937). Its structure is still not known. Recently we reported on the high-pressure synthesis, properties, and crystal structure of CrP_4 (Jeitschko & Donohue, 1972) and CrP_2 (Jeitschko & Donohue, 1973). We have now prepared at high pressure and characterized MnP_4, which forms Mn–Mn pairs. It is related to CrP_4 where the Cr atoms form continuous chains.

Preparation and properties

MnP_4 was prepared in a tetrahedral anvil press in a manner similar to that which we reported for CrP_4. High-purity (> 99·9 %) powders of Mn and red P, mixed in atomic ratios varying between 1 : 3 and 1 : 4, were subjected to temperatures of 1500–1700 K at pressures of 30–55 kbar. After 1–2 h at these conditions the samples were cooled over 1–2 h to 1300 K and quenched while still under pressure. Owing to a temperature gradient along the cylindrical pellet, black crystals grew at the ends of the container. Chemical analysis indicated the formula MnP_4. The center of the pellet gave X-ray powder patterns of MnP_4 plus diffraction lines of unidentified phases.

Electrical resistivity measurements with the four-probe technique on a crystal of unknown orientation showed semiconductor behavior with a room temperature resistivity of 30 ohm cm and an activation energy (from $\varrho=\varrho_0 \cdot e \exp E_a/kT$) of 0·14 eV. Magnetic measurements indicated diamagnetism.

* Contribution No. 2180.

Structure determination

Unit cell and space group

Single crystals of MnP_4, isolated from the quenched and crushed high-pressure samples, were investigated in a Buerger precession camera with Mo $K\alpha$ radiation. They show $2/m$ symmetry. Diffraction extinctions (hkl present only with $h+k=2n$; $h0l$ only with $l=2n$) are characteristic of space groups $C2/c$ and Cc, of which $C2/c$ was found to be correct during the structure determination.

A Guinier–Hägg powder photograph (Table 1), recorded at 298 K with Cu $K\alpha_1$ radiation and high-purity KCl ($a=6{\cdot}2931$ Å) as standard, was evaluated with a David–Mann film reader and indexed with the unit cell found from the single-crystal photographs. Least-squares refined lattice constants are: $a=10{\cdot}513$ (1), $b=5{\cdot}0944$ (4), $c=21{\cdot}804$ (2) Å, $\beta=94{\cdot}71$ (1)°, $V=1163{\cdot}8$ (1) Å^3. With the exact composition MnP_4 and 16 formula units per cell found during the structure determination, the calculated density is 4·082 g cm^{-3}, which compares well with the density of 4·09 g cm^{-3}, determined by displacement in bromoform.

Intensity data

The single crystal selected for the collection of the intensity data had irregular shape with overall exten-

sions varying between 42 and 65 μm. Zr-filtered Mo radiation was used with a four-circle automated diffractometer, scintillation counter, and pulse-height discriminator. Scans were over 1·0° in 2θ plus the angular separation of the $K\alpha$ doublet, with scan speed of 0·4° 2θ min^{-1}. Background was counted for 20 s at both ends of each scan. The intensity of a strong standard reflection varied $\pm 2{\cdot}0\%$ over the period of data collection. All reflections within the asymmetric quadrant up to 75° 2θ were measured. The usual Lorentz–polarization correction was applied. No absorption correction was made, since transmission values calculated for the extremes in crystal shape varied only between 74 and 83%. They correspond to relative errors of less than $\pm 2{\cdot}5\%$ in structure factors.

Table 1. *Evaluation of a Guinier–Hägg powder pattern of* MnP_4

Cu $K\alpha_1$ radiation; calculated data were generated by a computer program (Yvon, Jeitschko & Parthé, 1969) from the refined structure.

hk ℓ	d_c	d_o	I_c	I_o	hk ℓ	d_c	d_o	I_c	I_o	hk ℓ	d_c	d_o	I_c	I_o
00 2	10.865		<1		31 5	2.3293		3		42 0	1.8261		<1	
00 4	5.4326		1		02 5	2.3063	2.3078	4	vvw	-51 5	1.8222	1.8221	7	vvw
20 0	5.2388		<1		11 8	2.3006	2.3016	4	vvw	-42 2	1.8180	1.8174	8	vvw
-20 2	4.8783		1		22 0	2.2908		8		40 8	1.8126		3	
11 0	4.5816		4		40 4	2.2871	2.2868	3	vs	22 7	1.8124		6	
20 2	4.5743	4.5773	10	w	-22 1	2.2867		25		42 1	1.8111	1.8111	22	s
-11 1	4.5159	4.5133	34	vs	22 1	2.2697		<1		0012	1.8109		2	
11 1	4.4508		<1		-22 2	2.2579		1		-42 3	1.7953	1.7946	5	vw
-11 2	4.2769	4.2752	4	vvw	22 2	2.2254	•	8	•	-3110	1.7942		6	
11 2	4.1683	4.1659	14	w	-40 6	2.2104		<1		31 9	1.7916	1.7911	11	vs
-11 3	3.9364		2		-22 3	2.2071	2.2070	17	s	1111	1.7908		24	
-20 4	3.9360		<1		02 5	2.1976		<1		42 2	1.7843		3	
11 3	3.8107	3.8084	32	s	-31 7	2.1867	2.1853	6	m	-22 8	1.7830	1.7835	3	vvw
20 4	3.6252		<1		31 6	2.1836		6		51 4	1.7830		1	
00 6	3.6217		<1		0010	2.1730		<1		-51 6	1.7654		<1	
-11 4	3.5660		2		-11 9	2.1684	2.1682	18	m	-42 4	1.7617	1.7614	4	vvw
11 4	3.4419	3.4391	5	vvw	22 3	2.1619		<1		-2012	1.7566		<1	
-11 5	3.2112		<1		-22 4	2.1385		4		02 9	1.7523		1	
-20 6	3.1006		<1		11 9	2.1051		1		42 3	1.7472		<1	
11 5	3.0980		<1		22 4	2.0842	2.0843	3	vvw	-60 2	1.7468	1.7465	40	vs
-11 6	2.8922		<1		02 6	2.0835		<1		60 0	1.7463		<1	
-31 1	2.8812	2.8792	3	w	-2010	2.0682	2.0676	4	vvw	-4010	1.7443		<1	
31 0	2.8806		7		-22 5	2.0572	2.0564	3	vvw	51 5	1.7280		<1	
20 6	2.8709		<1		-31 8	2.0467		<1		22 8	1.7210	1.7209	5	vvw
-31 2	2.8323	2.8302	20	vvs	40 6	2.0442		<1		-42 5	1.7191		<1	
31 1	2.8308		54		31 7	2.0437		1		-1112	1.7052		1	
11 6	2.7928		1		22 5	1.9971	1.9969	7	vw	-60 4	1.7038		1	
-31 3	2.7412	2.7392	44	vvs	-1110	1.9913		<1		-51 7	1.7031		<1	
31 2	2.7388		18		02 7	1.9692		1		60 2	1.7024		3	
00 8	2.7163	2.7154	100	vvs	-22 6	1.9682	1.9686	3	vvw	42 4	1.7018		5	
-31 4	2.6195	2.6180	34	vs	-40 8	1.9680		1		-22 9	1.6925	1.6926	14	m
40 0	2.6194		1		2010	1.9513	1.9512	5	vvw	-3111	1.6832	1.6835	13	m
31 3	2.6165		1		-51 1	1.9434	1.9432	3	vvw	3110	1.6809	1.6810	19	s
-11 7	2.6139		<1		51 0	1.9380		1		13 0	1.6763		1	
-40 2	2.5955		<1		1110	1.9366	1.9365	9	w	-13 1	1.6730		1	
02 0	2.5472		1		-51 2	1.9334		1		2012	1.6697		<1	
02 1	2.5299		1		51 1	1.9175		<1		13 1	1.6696		<1	
11 7	2.5281		1		-31 9	1.9154		<1		-42 6	1.6695	1.6698	2	vvw
40 2	2.5001		<1		31 8	1.9126	1.9125	9	w	1112	1.6638		1	
-20 8	2.4967		<1		-51 3	1.9087		<1		-13 2	1.6600	1.6602	11	w
02 2	2.4800		1		22 6	1.9053		1		51 6	1.6572		1	
-31 5	2.4797	2.4794	1	vvw	51 2	1.8833		<1		13 2	1.6534		<1	
31 4	2.4765		<1		-22 7	1.8757		<1		0210	1.6532		<1	
-40 4	2.4391		2		-51 4	1.8708		1		42 5	1.6502	1.6505	3	vvw
02 3	2.4030	2.4031	9	w	02 8	1.8580		<1		-13 3	1.6378	1.6381	13	m
-11 8	2.3742	2.3735	6	vw	-1111	1.8382		1		-51 8	1.6375		1	
20 8	2.3344		<1		51 3	1.8376	1.8376	7	vw	22 9	1.6328		1	
-31 6	2.3328	2.3324	7	w	-42 1	1.8286	1.8279	20	s	11 3	1.6284		1	

*Coincidence KCl

Solution and refinement of the structure

The Patterson synthesis, computed with a program by Fritchie & Guggenberger (1967), showed maxima at $z \approx 0, \frac{1}{8}, \frac{2}{8}, \frac{3}{8}$, *etc.* Thus it was concluded that the structure contains layers separated from each other by approximately $\Delta z = \frac{1}{8}$. The correspondence of the cell dimensions a and b of CrP_4 (Jeitschko & Donohue, 1972) with b and a of MnP_4 was noted, and the similarity (but not equivalence) of the Patterson functions of CrP_4 and MnP_4 at $z \approx 0$ suggested a close relationship between the two structures. Of further help was our expectation that the Mn atoms would form pairs. With the aid of models it was found that there are two basically different ways of connecting adjacent CrP_4-like layers. One mode of linking is compatible with short or long metal–metal interactions and the other does not allow for metal–metal bonds. The correct structure, which was arrived at by trial and error using both possible space groups and successive least-squares refinements of partial structures and difference Fourier syntheses, combines all three kinds of interfaces between adjacent layers.

The structure was refined with a full-matrix least-squares program by Finger (1969). The sum $\sum w_i(KF_o - |F_c|)^2$ was minimized, where w_i is the weight based on counting statistics, and K the scale factor. Atomic scattering values for neutral atoms were taken from Cromer & Mann (1968), corrected for anomalous dispersion (Cromer & Liberman, 1970). Zachariasen's (1963) correction for secondary extinction was used. Structure factors for which this correction amounted to more than 10%, as well as structure factors which were smaller than three times their standard deviations, were given zero weight. Final conventional R values for the refinement with isotropic thermal parameters are 0·056 for 1765 reflections with nonzero weight and 0·112 for the total of 3036 reflections. For the refinement with anisotropic thermal parameters, the corresponding R values are 0·051 and 0·109. Parameters obtained in this

Table 2. *Positional and thermal parameters of* MnP_4

All atoms are in the general position of $C2/c$. Numbers in parentheses are e.s.d.'s in the least significant digits. Vibrational parameters ($\times 10^5$) are defined through $T = \exp(-\sum\sum h_i h_j \beta_{ij})$. The last column contains equivalent isotropic B values. They agree (within their standard deviations) with the values obtained in the least-squares refinement with isotropic thermal parameters.

	x	y	z	β_{11}	β_{22}	β_{33}	β_{12}	β_{13}	β_{23}	B(Å^2)
Mn(1)	0·92576 (9)	0·1172 (2)	0·07002 (4)	62 (6)	227 (31)	10 (1)	−24 (11)	−5 (2)	2 (5)	0·23 (1)
P(1)	0·57712 (16)	0·3274 (3)	0·03698 (7)	116 (12)	200 (53)	13 (3)	36 (19)	−9 (4)	−7 (9)	0·33 (2)
P(2)	0·76977 (16)	0·4090 (3)	0·08340 (7)	90 (11)	296 (51)	16 (3)	−13 (19)	−16 (4)	21 (9)	0·34 (2)
P(3)	0·07973 (16)	0·4207 (3)	0·07441 (7)	126 (11)	137 (50)	14 (3)	−15 (19)	−5 (4)	0 (9)	0·32 (2)
P(4)	0·77567 (16)	0·8099 (3)	0·04916 (7)	105 (12)	262 (52)	11 (3)	−17 (19)	−7 (4)	4 (9)	0·32 (2)
Mn(2)	0·31551 (9)	0·8018 (2)	0·18209 (4)	60 (7)	256 (30)	8 (1)	−26 (11)	−7 (2)	2 (5)	0·23 (1)
P(5)	0·47458 (15)	0·5175 (3)	0·17056 (7)	87 (11)	203 (49)	17 (3)	30 (19)	−3 (4)	7 (9)	0·31 (2)
P(6)	0·17128 (16)	0·1223 (3)	0·21538 (7)	83 (11)	239 (49)	22 (3)	35 (20)	−11 (4)	4 (9)	0·35 (2)
P(7)	0·16026 (16)	0·5081 (3)	0·16917 (8)	92 (11)	356 (52)	13 (3)	−31 (19)	−3 (4)	−9 (9)	0·35 (2)
P(8)	0·46793 (16)	0·1058 (3)	0·19999 (7)	103 (11)	288 (52)	16 (2)	63 (20)	−5 (4)	6 (9)	0·36 (2)

refinement* are listed in Table 2. Within their standard deviations, positional parameters are the same in the refinements with isotropic and anisotropic thermal parameters. The ratio of the long to the short axis of the thermal ellipsoids varies between 1·35 [Mn(1)] and 2·6 [P(2)]. These ellipsoids are somewhat affected by errors in the data due to absorption. The low R values of 0·044 (isotropic) and 0·039 (anisotropic thermal parameters) for the 1366 strongest reflections indicate better the accuracy of the structure determination than the overall R values given above, which are strongly affected by the large number of weak reflections with poor counting statistics.

* A list of structure factors has been deposited with the British Library Lending Division as Supplementary Publication No. SUP 30692 (17 pp., 1 microfiche). Copies may be obtained through The Executive Secretary, International Union of Crystallography, 13 White Friars, Chester CH1 1NZ, England.

Description of the structure and comparison with CrP_4

The crystal structure of MnP_4 is best described as a layer structure although bonding within and between the layers is of equal strength. The layers are all of the same kind (disregarding slight differences in bond

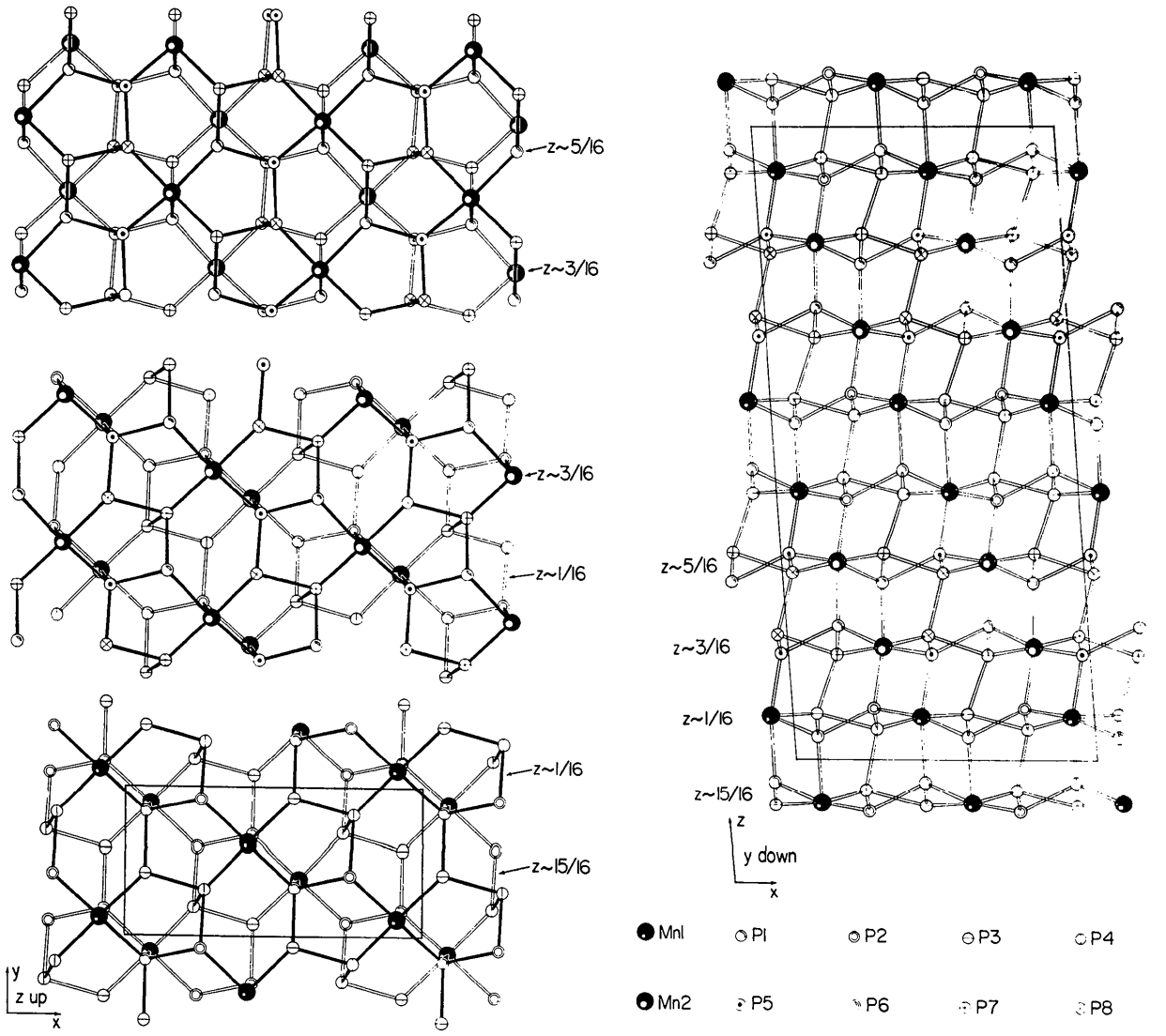

Fig. 1. Normal projections of the MnP_4 structure. On the right-hand side the atomic layers at $z\sim\frac{15}{16}$, $\frac{1}{16}$, $\frac{3}{16}$, *etc.*, are shown from the side. Each layer contains either Mn(1) or Mn(2) atoms. The three types of interfaces between adjacent layers are shown on the left-hand side. They allow for Mn(1)–Mn(1), Mn(1)–Mn(2), and Mn(2)–Mn(2) interactions. Only the interaction Mn(1)–Mn(2) is bonding. In spite of the appearance in the projections, the P_6 octahedra around Mn(2) atoms of adjacent layers (*e.g* at $z\sim\frac{3}{16}$ and $\frac{5}{16}$) do not share edges but corners.

distances and angles) with one Mn and four P atoms forming a puckered tessellation of pentagons and hexagons. The layers at $z\sim\frac{15}{16}$ and $\frac{1}{16}$ (Fig. 1) correspond to the two-layer structure of CrP_4 (Jeitschko & Donohue, 1972). In MnP_4 eight layers of different orientation and connectivity are needed to complete one unit cell. The four subsequent layers at $z\sim\frac{13}{16}$, $\frac{15}{16}$, $\frac{1}{16}$, and $\frac{3}{16}$ are parallel to each other. The subsequent four layers at $z\sim\frac{5}{16}$, $\frac{7}{16}$, $\frac{9}{16}$, and $\frac{11}{16}$ are also parallel to each other, but, relative to the adjacent layers above and below, rotated 180° around an axis perpendicular to the layers. This can best be seen by comparing the inclination of MnP_6 octahedra of adjacent layers (Fig. 2).

The two independent Mn atoms are in approximately octahedral coordination to P atoms. The Mn atoms of four adjacent parallel layers together with their P neighbors form a group of four edge-sharing MnP_6 octahedra, which are connected to other MnP_6 octahedra above and below by corners. Within the group of four edge-sharing MnP_6 octahedra there are two short Mn(1)–Mn(2) interactions (Fig. 3). Bonding distances Mn–P vary from 2·215 to 2·380 Å with average distances of 2·278 Å for Mn(1) and 2·286 Å for Mn(2). Those P–Mn–P angles which in a regular octahedron are 90°, vary between 74 and 99°.

The eight independent P atoms are all in more or less distorted tetrahedral coordination. P(1), P(2), P(5), and P(6) are coordinated to 2 Mn and 2 P atoms. The other four P atoms each have 1 Mn neighbor and 3 P neighbors. Tetrahedral bond angles Mn–P–P and

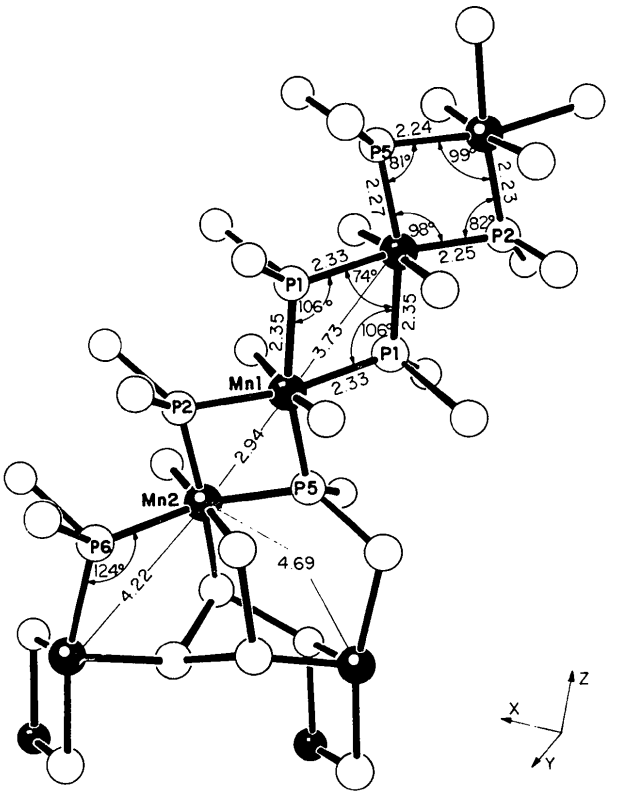

Fig. 3. Near-neighbor environments of the Mn atoms in MnP_4.

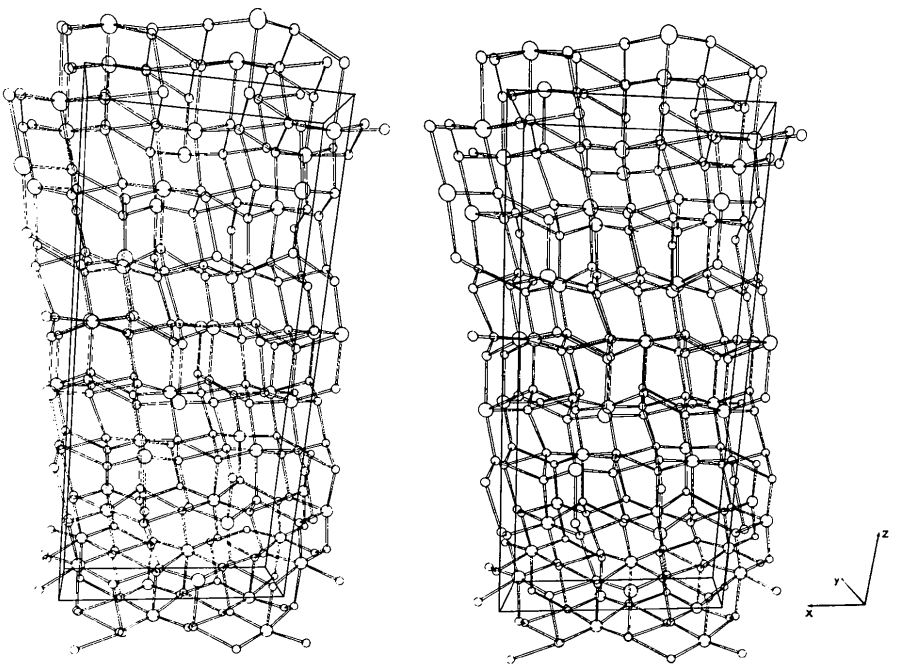

Fig. 2. Stereo drawing of the MnP_4 structure. The Mn atoms are drawn as large spheres.

P–P–P vary from 94 to 130° and from 89 to 106°, respectively. The four different Mn–P–Mn angles are shown in Fig. 3. P–P distances cover the range from 2·177 to 2·278 Å. The average P–P distance of 2·225 Å agrees well with the average P–P distances of 2·21 ± 0·02 Å in elemental P modifications (Brown & Rundqvist, 1965; Thurn & Krebs, 1969), in CdP_4 (Krebs, Müller & Zürn, 1956), in TlP_5 (Olofsson & Gullmann, 1971), and in alkali and earth alkali polyphosphides as Na_3P_{11} (Wichelhaus & von Schnering, 1973), Sr_3P_{14} (Dahlmann & von Schnering, 1972), and SrP_3 (Dahlmann & von Schnering, 1973).

The average P–P distance of 2·213 Å in CrP_4 is slightly smaller than the average P–P distance of 2·225 Å in MnP_4. This is probably due to larger deviations from ideal P–P bonding distances in MnP_4.* Average isotropic thermal parameters in CrP_4 and MnP_4 are very similar with 0·27 and 0·35 $Å^2$ for Cr and P in CrP_4, and 0·23 and 0·34 $Å^2$ for Mn and P in MnP_4. Systematic errors in these values, due to systematic differences in the absorption of low- and high-angle reflections (which were not corrected for), were calculated to be less than 0·01 $Å^2$.

The rationalization of the MnP_4 and CrP_4 structures as stacking variants of one net, allows one to predict structures with other stacking sequences for binary and ternary compounds TX_4, depending on the bonding requirements of the transition metal (T) and metalloid (X) atoms, as is known for compositions TX_2 with pyrite, marcasite, PdP_2, PdS_2, PdPS, and $AuSn_2$ (α-$NiAs_2$) type structures (Jeitschko, 1974).

* In a solid-state compound generally not all bonding distances can be optimized. Since free energy *versus* bond distance curves are steeper for deviations in shorter than in longer distances, the *average* distances will be greater for structures with greater deviations from ideal bonding distances. This effect corresponds to the well known thermal expansion. There the deviations from ideal bonding distances are dynamic, of course.

Table 3. *Interatomic distances in* MnP_4 (Å)

Standard deviations, computed from e.s.d.'s of positional parameters and lattice constants, are all less than 0·003 Å. All distances shorter than 3·6 Å (for Mn) and 2·8 Å (for P atoms) are listed.

Mn(1)–P(1)	2·326	Mn(2)–P(2)	2·234
–P(1)	2·347	–P(5)	2·241
–P(2)	2·249	–P(6)	2·380
–P(3)	2·235	–P(6)	2·409
–P(4)	2·243	–P(7)	2·215
–P(5)	2·268	–P(8)	2·240
–Mn(2)	2·941	–Mn(1)	2·941
P(1)—Mn(1)	2·326	P(5)—Mn(1)	2·268
–Mn(1)	2·347	–Mn(2)	2·241
–P(2)	2·229	–P(6)	2·278
–P(3)	2·226	–P(8)	2·196
P(2)—Mn(1)	2·249	P(6)—Mn(2)	2·380
–Mn(2)	2·234	–Mn(2)	2·409
–P(1)	2·229	–P(5)	2·278
–P(4)	2·177	–P(7)	2·207
P(3)—Mn(1)	2·235	P(7)—Mn(2)	2·215
–P(1)	2·226	–P(3)	2·214
–P(4)	2·246	–P(6)	2·207
–P(7)	2·214	–P(8)	2·237
P(4)—Mn(1)	2·243	P(8)—Mn(2)	2·240
–P(2)	2·177	–P(5)	2·196
–P(3)	2·246	–P(7)	2·237
–P(4)	2·252	–P(8)	2·230

Bonding in MnP_4 and CrP_4

In a qualitative valence-bond description sp^3 and d^2sp^3 hybridization can be assumed for the P and Mn atoms, respectively. Ascribing two electrons to each of the short Mn–P and P–P interactions, the Mn atoms obtain a d^5 system (oxidation number 2+). The same result is arrived at by assigning oxidation number zero to each P atom bonded to 3 P and 1 Mn, and oxidation number 1− to each P bonded to 2 P and 2 Mn atoms. Two nonbonding electrons can be accommodated in each of two t_{2g} orbitals while the fifth electron occupies the third t_{2g} orbital and forms a bond with the corresponding electron of one neighboring Mn atom. This results in the formation of Mn(1)–Mn(2) pairs in agreement with the diamagnetic behavior of the compound.

The Mn(1)–Mn(2) distance of 2·94 Å is rather long for a bonding distance when compared to the 'normal' single-bond distance of 2·4 Å, but the distortions in bond angles (tetrahedral angles are reduced from 109 to 81 and 82°, octahedral angles are widened from 90 to 98 and 99°) clearly indicate the bonding Mn(1)–Mn(2) interaction (Fig. 3). If the electrons in the Mn–P bonds are counted as one belonging to Mn and the other one to P, the Mn atoms obtain a formal charge of 4−. Although the actual charge distribution is not known, electrostatic repulsion may also contribute to the stretching of the Mn(1)–Mn(2) bond. The latter argument was used to explain the unexpected length of the Mn–Mn bond of 2·92 Å in $Mn_2(CO)_{10}$ (Dahl & Rundle, 1963). There, of course, the bonding Mn–Mn interaction is indisputable, since there are no other bonds between the Mn atoms. For the same reason no superexchange mechanism is possible, and by analogy, does not need to be invoked for MnP_4. Metal–metal bonding, indicated by distortions of near-neighbor environments, occurs for distances as long as 3·31 Å, as was found in NbI_4 (Dahl & Wampler, 1962). The fact that the MnP_6 octahedra are linked by edges is additional evidence for Mn–Mn bonding, since linking by corners is favoured for electrostatic reasons, as long as the Mn–P bonds have some polarity. Corner-sharing is geometrically possible, as demonstrated by CdP_4 and it occurs even for compositions with lower metalloid (X) content as in the large number of compounds with skutterudite (TX_3) and pyrite (TX_2) type structure.

Near-neighbor distortions and diamagnetism or Pauli paramagnetism* also indicated metal–metal

* The method employed was not sensitive enough to distinguish between the two.

bonding in CrP_4, where Cr^{2+} with low spin d^4 configuration is also in octahedral P environment and the CrP_6 octahedra share edges to form zigzag chains with Cr–Cr bonding distances of 3·18 Å (Jeitschko & Donohue, 1972). There, as in MnP_4, the optimization of all bonding interactions seems not possible for geometric reasons.*

A comparison of the MnP_4 structure with the structure of CrP_4 allows one to rationalize why CrP_4 is a metal, while MnP_4 is a semiconductor. In accordance with bonding descriptions given by Bither, Bouchard, Cloud, Donohue & Siemons (1968) for TX_2 compounds (T = transition metal, X = S, Se, Te) with pyrite structure, we assume the d levels of the metal atoms in MnP_4 and CrP_4 to be located between the bonding and antibonding T–P and P–P bonds (Fig. 4). The relatively long Cr–Cr distances of 3·18 Å in CrP_4 allow only weak bonding and band splitting. Consequently the bonding and antibonding Cr–Cr d functions overlap, giving rise to metallic conductivity. In MnP_4 the Mn–Mn bond is shorter (2·94 Å). This results in stronger Mn–Mn bonds and larger splitting of bonding and antibonding d bands. If the splitting is large enough a band gap develops as shown in Fig. 4; however, even if those bands are not completely separated in energy, MnP_4 could be semiconducting simply because the Mn–Mn interactions are not continuous throughout the structure.

The kind of metal–metal bonding in CrP_4 with continuous zigzag chains of edge-sharing octahedra is also found in β-ReO_2 (Magnéli, 1957). Pairing of metal atoms across edges of edge-sharing octahedra as found in MnP_4 also occurs in several transition-metal oxides and halides, *e.g.* NbO_2 and $NbCl_4$ (Schäfer & von Schnering, 1964). In all these compounds, it is generally agreed that the short metal–metal distances represent bonding metal–metal interactions. Thus metal–metal pairs are formed by single bonds in NbO_2 and by double bonds in MoO_2 (Rogers, Shannon, Sleight & Gillson, 1969).

* A direct proof and elaboration of this statement could be accomplished by least-squares and angles refinements as discussed by Shoemaker & Shoemaker (1967), Meier & Villiger (1969), and Baur (1971).

Marcasites and arsenopyrites

The short metal–metal distances in CrP_4 and MnP_4 have their counterparts in the large number of compositions TX_2 with arsenopyrite and loellingite structure (Hulliger, 1968) where the short metal–metal distances also occur across edges of edge-sharing octahedra. In the arsenopyrites (where the metal atoms have a d^5 configuration), pairing of the metal atom occurs, as is the case for the Mn atoms in MnP_4 which also have d^5 configuration. In the loellingites (= marcasites with the T atoms in d^2 and d^4 configuration) the metal atoms form continuous straight strings, while continuous zigzag chains are formed for Cr atoms (d^4) in CrP_4.

Several conflicting bonding models have been suggested for the arsenopyrites and marcasites. A detailed review of these models will not be given here and the reader is referred to the original papers (Hulliger & Mooser, 1965; Pearson, 1965; Brostigen & Kjekshus, 1970; Goodenough, 1972). It is, however, remarkable that not one of the more recent bonding models allows for metal–metal bonding in the loellingites, quite in contrast with the generally accepted view that short interatomic distances indicate bonding, especially when alternate structures are competing (as is the pyrite structure in this case), where the short nonbonding interactions could be avoided.

We therefore propose yet another model which has σ and π metal–metal bonding in the d^2 and d^4 marcasites and σ metal–metal bonds in the (d^5) arsenopyrites. It requires the usual mixing of the d_{x2-y2}, d_{z2}, s, and p^3 states to form σ bonds to the octahedrally surrounding X atoms. The (say) d_{xy} orbital is then σ bonding with the neighboring metal atoms. A linear combination of the remaining d_{xz} and d_{yz} orbitals results in one orbital which is nonbonding with respect to metal neighbors and one orbital which is π bonding with the corresponding orbitals of the neighboring metal atoms. In this way each T atom forms two σ and two π T–T half-bonds in the d^2 and d^4 marcasites, thus accounting for the short c axis in these marcasites. In the arsenopyrites the metal atoms have d^5 configuration and only one (σ) metal–metal bond can be formed per T atom, resulting in T–T pairing. For the d^6 marcasites no

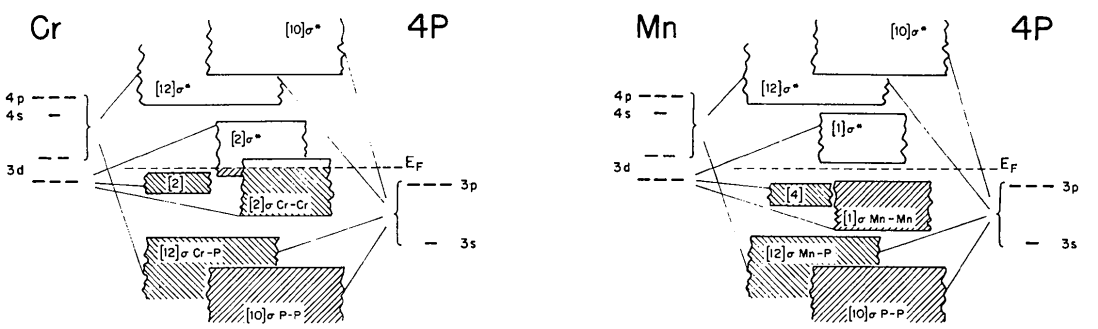

Fig. 4. Schematic MO energy-level diagrams for CrP_4 and MnP_4. Numbers in brackets refer to states per formula unit.

metal–metal bonding exists as was also assumed in previous bonding proposals, and the c axis is therefore greater in the d^6 marcasites than in the d^4 marcasites.*

The present model differs from the one proposed by Goodenough (1972) mainly in the relative position of bonding and nonbonding t_{2g} levels above and below the Fermi level. Thus conductive and magnetic properties are similar for both models and our model agrees well with the experimental findings for $FeAs_2$, $FeSb_2$ (Fan, Rosenthal, McKinzie & Wold, 1972), and $FeAs_{2-x}Se_x$ (Baghdadi & Wold, 1974).

We are indebted to C. G. Frederick and J. L. Gillson for magnetic and electric conductivity measurements, and C. L. Hoover for supervision of the high-pressure experiments. C. M. Foris and D. M. Graham gave competent help with the crystallographic work.

* Table I of the paper by Brostigen & Kjekshus (1970) lists a d^0 defect marcasite $Mo_{2/3}As_2$ with short c axis. This compound seems to contradict our bonding proposal [but might be considered as supporting Goodenough's (1972) model] since a long c axis would be expected for a d^0 compound where no T–T bonds are possible. However, bonding in a defect structure is certainly quite different from that in a compound with stoichiometry TX_2. Furthermore, this compound, reported with composition $Mo_{0.4}As_2$ by Brown (1965), could not be confirmed in subsequent investigations of the Mo–As system by Taylor, Calvert & Hunt (1965) and Jensen, Kjekshus & Skansen (1966).

References

BAGHDADI, A. & WOLD, A. (1974). *J. Phys. Chem. Solids*, **35**, 811–815.

BAUR, W. H. (1971). *Nature Phys. Sci.* **233**, 135–137.

BILTZ, W., WIECHMANN, F. & MEISEL, K. (1937). *Z. anorg. allgem. Chem.* **234**, 117–129.

BITHER, T. A., BOUCHARD, R. J., CLOUD, W. H., DONOHUE, P. C. & SIEMONS, W. J. (1968). *Inorg. Chem.* **7**, 2208–2220.

BROSTIGEN, G. & KJEKSHUS, A. (1970). *Acta Chem. Scand.* **24**, 2993–3012.

BROWN, A. (1965). *Nature, Lond.* **206**, 502–503.

BROWN, A. & RUNDQVIST, S. (1965). *Acta Cryst.* **19**, 684–685.

CROMER, D. T. & LIBERMAN, D. (1970). *J. Chem. Phys.* **53**, 1891–1898.

CROMER, D. T. & MANN, J. B. (1968). *Acta Cryst.* A**24**, 321–324.

DAHL, L. F. & RUNDLE, R. E. (1963). *Acta Cryst.* **16**, 419–426.

DAHL, L. F. & WAMPLER, D. L. (1962). *Acta Cryst.* **15**, 903–911.

DAHLMANN, W. & VON SCHNERING, H. G. (1972). *Naturwissenschaften*, **59**, 420.

DAHLMANN, W. & VON SCHNERING, H. G. (1973). *Naturwissenschaften*, **60**, 429.

FAN, A. K. L., ROSENTHAL, G. H., MCKINZIE, H. L. & WOLD, A. (1972). *J. Solid State Chem.* **5**, 136–143.

FINGER, L. W. (1969). Unpublished computer program for the least-squares refinement of crystal structures.

FRITCHIE, C. J. JR & GUGGENBERGER, L. J. (1967). Unpublished electron summation program.

GOODENOUGH, J. B. (1972). *J. Solid State Chem.* **5**, 144–152.

HULLIGER, F. (1968). *Struct. Bond.* **4**, 83–229.

HULLIGER, F. & MOOSER, E. (1965). In *Progress in Solid State Chemistry*, edited by H. REISS, Vol. 2, pp. 330–377. New York: Pergamon Press.

JEITSCHKO, W. (1974). *Acta Cryst.* B**30**, 2565–2572.

JEITSCHKO, W. & DONOHUE, P. C. (1972). *Acta Cryst.* B**28**, 1893–1898.

JEITSCHKO, W. & DONOHUE, P. C. (1973). *Acta Cryst.* B**29**, 783–789.

JENSEN, P., KJEKSHUS, A. & SKANSEN, T. (1966). *Acta Chem. Scand.* **20**, 403–416.

KREBS, H., MÜLLER, K.-H. & ZÜRN, G. (1956). *Z. anorg. allgem. Chem.* **285**, 15–28.

MAGNÉLI, A. (1957). *Acta Chem. Scand.* **11**, 28–33.

MEIER, W. M. & VILLIGER, H. (1969). *Z. Kristallogr.* **129**, 411–423.

OLOFSSON, O. & GULLMAN, J. (1971). *Acta Chem. Scand.* **25**, 1327–1337.

PEARSON, W. B. (1965). *Z. Kristallogr.* **121**, 449–462.

ROGERS, D. B., SHANNON, R. D., SLEIGHT, A. W. & GILLSON, J. L. (1969). *Inorg. Chem.* **8**, 841–849.

RUNDQVIST, S. (1962). *Ark. Kem.* **20**, 67–113.

SCHÄFER, H. & VON SCHNERING, H. G. (1964). *Angew. Chem.* **76**, 833–849.

SHOEMAKER, C. B. & SHOEMAKER, D. P. (1967). *Acta Cryst.* **23**, 231–238.

TAYLOR, J. B., CALVERT, L. D. & HUNT, M. R. (1965). *Canad. J. Chem.* **43**, 3045–3051.

THURN, H. & KREBS, H. (1969). *Acta Cryst.* B**25**, 125–135.

WICHELHAUS, W. & VON SCHNERING, H. G. (1973). *Naturwissenschaften*, **60**, 104.

YVON, K., JEITSCHKO, W. & PARTHÉ, E. (1969). *A Fortran IV Program for the Intensity Calculation of Powder Patterns*. Report of the LRSM Laboratory, Univ. of Pennsylvania, Philadelphia, Pa.

ZACHARIASEN, W. H. (1963). *Acta Cryst.* **16**, 1139–1144.

ÅRSTAD, O. & NOWOTNY, H. (1937). *Z. phys. Chem.* B**38**, 356–358.